

# Novel Collider Signatures for Little Higgs Dark Matter Models

Chian-Shu Chen <sup>\*</sup>, Kingman Cheung <sup>†</sup>, and Tzu-Chiang Yuan <sup>‡</sup>

*Department of Physics and NCTS, National Tsing Hua University, Hsinchu, Taiwan*

(Dated: October 12, 2018)

## Abstract

Little Higgs models with  $T$ -parity provide a stable neutral particle  $A_H$ , the lightest  $T$ -odd particle (LTP), which was recently proposed to explain the cold dark matter of the Universe. In the coannihilation region of the LTP with the Little Higgs partner of the light quark  $Q_H$ , we propose novel signatures for its detection at hadronic colliders by searching for monojet and dijet plus missing energy events due to the associated production of  $Q_H A_H$  and direct production of  $Q_H \bar{Q}_H$ , respectively. Using the most recent WMAP data, we show that the coupling of  $A_H$ - $Q_H$ - $q$  is tightly constrained in the coannihilation region. This implies that the monojet signal is too small to be discernible but the dijet plus missing energy signal is potentially measurable at the LHC.

---

<sup>\*</sup> Email address: d927305@oz.nthu.edu.tw

<sup>†</sup> Email address: cheung@phys.nthu.edu.tw

<sup>‡</sup> Email address: tcyuan@phys.nthu.edu.tw

## I. INTRODUCTION

Recent studies on cosmology have almost unanimously confirmed the existence of dark matter (DM) in our Universe with a fraction  $\Omega_{DM} \simeq 0.22$  of the critical density [1]. However, the identity of the DM still remains to be a mystery. Future DM direct and indirect detection experiments and collider experiments will attempt to pin down the properties of the DM candidates and the underlying theories. Among various proposed candidates in the literature, the most studied one is the lightest supersymmetric particle (LSP, usually the lightest neutralino) of supersymmetric theories (SUSY). Recently, another class of models based on Little Higgs models [2] imposed with a  $T$ -parity [3, 4, 5] provides an alternative DM candidate. In these models, all the standard model particles are assigned with an even  $T$ -parity, while all the new particles proposed are assigned with an odd  $T$ -parity, except for the Little Higgs partner of the top quark. Because of the  $T$ -parity assignment the lightest  $T$ -odd particle (LTP) is stable and hence a potential candidate to account for the DM of the Universe [6, 7, 8]. We note that electroweak precision measurements have placed severe constraints on earlier attempts of constructing the Little Higgs models without  $T$ -parity [9]. Imposing a discrete  $T$ -parity in the Little Higgs models therefore opens a much wider window for theorists to explore various phenomenologies of this class of models [10].

In Little Higgs models with  $T$ -parity, the LTP is usually the  $A_H$ , the corresponding heavy Little Higgs partner of the  $B$  field of the  $U(1)_Y$  symmetry.<sup>1</sup> It has been shown [6, 8] that in order for the LTP to account for all the DM of the Universe, the mass  $M_{A_H}$  of  $A_H$  is related to the Higgs boson mass  $m_H$  by [8]

$$m_H \approx 24 + 2.38M_{A_H} \quad \text{or} \quad m_H \approx -83 + 1.89M_{A_H} . \quad (1)$$

This mass relation between  $m_H$  and  $M_{A_H}$  clearly indicates that the dominant annihilation channel is via an  $s$ -channel Higgs boson:  $A_H A_H \rightarrow h^{(*)} \rightarrow b\bar{b}, \tau^+\tau^-, W^+W^-, ZZ$ . Twice the mass of  $A_H$  must be located at either side of the Higgs boson peak,  $2M_{A_H} \approx m_H + \Delta$ . If  $2M_{A_H}$  is located right at the Higgs boson mass, the annihilation would be too strong to provide a sufficient relic density for the DM. Therefore,  $2M_{A_H}$  must fall on either side of the

---

<sup>1</sup> The  $A_H$  and  $Z_H$  fields are the mass eigenstates of  $B_H$  and  $W_H^0$  fields after a rotation by an angle analogous to the Weinberg angle, but the rotation in the present case is highly suppressed by  $v/f$ , where  $f \sim 1$  TeV is the high scale where  $[SU(2) \times U(1)]^2 \rightarrow SU_L(2) \times U_Y(1)$  in the Little Higgs models and  $v \sim 246$  GeV is the VEV to break  $SU_L(2) \times U_Y(1) \rightarrow U_{em}(1)$ . Thus,  $A_H$  is very close to  $B_H$ .

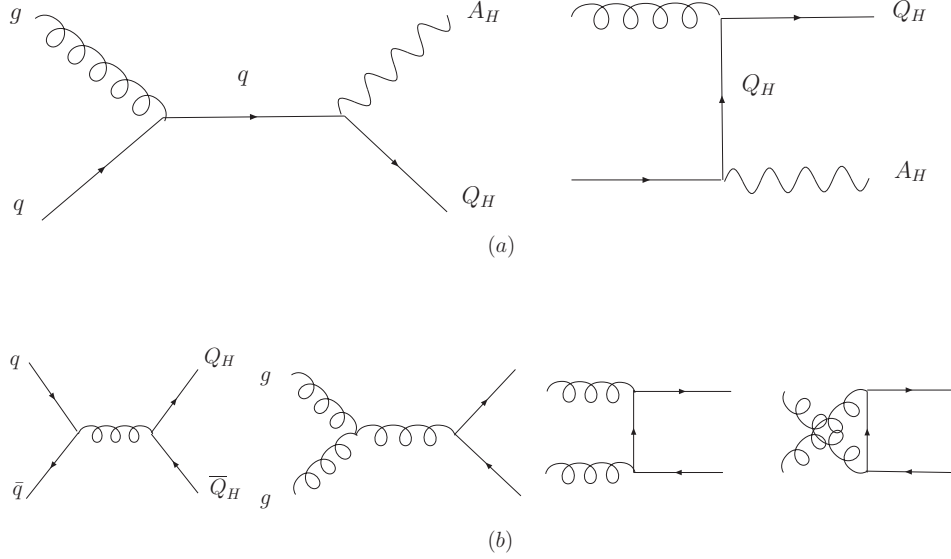


FIG. 1: Feynman diagrams for (a) production and coannihilation of  $A_H Q_H$  and (b) production and coannihilation of  $Q_H \bar{Q}_H$ . Production reads from left to right, whereas coannihilation reads from right to left.

Higgs boson mass such that the annihilation cross section has just the right size to produce the correct relic density for DM. This is somewhat a fine-tuned mechanism. Perhaps a slightly more natural domain of the parameter space is a region where the coannihilation of the LTP  $A_H$  and the  $T$ -odd partner of light quark  $Q_H$  becomes strong. This coannihilation region has been explored and is given by [8]

$$M_{A_H} + 20 \approx M_{Q_H} \quad , \quad (2)$$

with  $M_{Q_H} \geq 200$  GeV. Note that no mass relation is necessary for  $m_H$  and  $M_{A_H}$  in this coannihilation region. In this work, we consider that the coannihilation region is a more natural setting and we focus on the physics of this interesting region.

The Feynman diagrams responsible for coannihilation is depicted in Fig. 1. It has been widely discussed in the literature that the LHC is a good place to investigate the nature of the DM candidate. In this work, we propose novel signatures for the LTP of the Little Higgs models with  $T$ -parity in the coannihilation region. We consider the associated production of  $pp \rightarrow A_H Q_H$ , followed by the decay  $Q_H \rightarrow q A_H$ , which will give rise to monojet plus missing energy events, as well as the direct production of  $Q_H \bar{Q}_H$ , which gives rise to the dijet plus missing energy signal.

One can argue that using monojet plus missing energy events one can at least partially distinguish Little Higgs models with  $T$ -parity from minimal SUSY models with  $R$ -parity. Some of the reasons are (i) monojet events arising from  $gq \rightarrow \tilde{q}\tilde{\chi}_1^0$ , followed by  $\tilde{q} \rightarrow \tilde{\chi}_1^0 q$  with the lightest neutralino  $\tilde{\chi}_1^0$  as the LSP, is expected to be suppressed by the coupling. Thus, the dominant channels for producing SUSY particles are QCD production of  $\tilde{g}\tilde{g}$ ,  $\tilde{q}\tilde{q}^*$ , and  $\tilde{g}\tilde{q}(\tilde{q}^*)$ . They tend to give multijet ( $> 2$ ) plus missing energy events; (ii) the dominant mechanism for producing  $T$ -odd particles are  $qg \rightarrow A_H Q_H$ ,  $\bar{q}g \rightarrow A_H \bar{Q}_H$ , and  $gq, q\bar{q} \rightarrow Q_H \bar{Q}_H$ , which give rise to monojet and dijet, respectively, plus missing energy events. Therefore, by counting how many jets in multijet plus missing energy events, one may be able to differentiate between Little Higgs models with  $T$ -parity and minimal SUSY models. Note that it is possible to have some corners of parameter space in minimal SUSY models such that monojet plus missing energy events become discernible in SUSY, but the chance is very odd albeit not zero.<sup>2</sup>

Our analysis of relic density in Sec. III shows that the coupling of  $A_H$ - $Q_H$ - $q$  has to be rather small, such that the monojet plus missing energy signal is negligible compared with the Standard Model (SM) background. Nevertheless, the dijet plus missing energy signal via direct  $Q_H \bar{Q}_H$  production is comparable with the SM background. Potentially, the dijet signal is feasible at the LHC.

We organize our paper as follows. In the next Section, we list the formulas for the parton processes involved in our calculation. In Sec. III, we use the most recent WMAP result of the constrained DM cross section to obtain a suitable range for the coupling of  $A_H$ - $Q_H$ - $q$ . In Sec. IV, we calculate the monojet and dijet plus missing energy signals at hadronic colliders. Comparison of the predictions with the SM backgrounds are also discussed in this Section. We conclude in Sec. V.

## II. PARTON PROCESSES FOR PRODUCTION OF $A_H Q_H$ AND $Q_H \bar{Q}_H$

The relevant interaction Lagrangian density for the vertex  $A_H$ - $Q_H$ - $q$  is given by [8, 11]

$$\mathcal{L} = g_H \bar{Q}_H \gamma_\mu P_L q A_H^\mu + \text{H.c.}, \quad (3)$$

---

<sup>2</sup> If the mass difference between the squarks and the lightest neutralino is large, the monojet and dijet arising from SUSY tend to have a harder  $p_T$  spectrum than those coming from the  $Q_H$  decays in the coannihilation region of the Little Higgs models.

where the color indices for  $Q_H$  and  $q$  are suppressed, and  $g_H$  is the coupling constant to be determined. The QCD interaction of  $Q_H$  with the gluon fields is the same as that of the light quark  $q$ .

**A.  $qg \rightarrow A_H Q_H$  and  $\bar{q}g \rightarrow A_H \bar{Q}_H$**

There are two Feynman diagrams, depicted in Fig. 1(a), contributing to this process. Summing over the spins and colors of the initial and final state particles, the amplitude squared for the process  $q(p_1) g(p_2) \rightarrow A_H(k_1) Q_H(k_2)$  is given by

$$\begin{aligned} \sum |M|^2 = & 8g_H^2 g_s^2 \left\{ -\frac{1}{\hat{s}} \left( \hat{t}_Q + \frac{\hat{s}_{AQ} \hat{u}_A}{M_{A_H}^2} \right) \right. \\ & - \frac{1}{\hat{t}_Q^2} \left[ 2\hat{t}_A (\hat{s}_{AQ} + \hat{u}_Q) + 12M_{Q_H}^2 \hat{t}_A - (M_{A_H}^2 - M_{Q_H}^2) \hat{u}_Q \right. \\ & + \frac{\hat{t}_A}{M_{A_H}^2} (4M_{Q_H}^2 \hat{t}_A + \hat{u}_Q \hat{t}_A + M_{Q_H}^2 \hat{s}_{AQ}) \Big] \\ & - \frac{1}{\hat{s} \hat{t}_Q} \left[ \left( 1 + \frac{\hat{t}_A}{M_{A_H}^2} \right) (\hat{u}_Q \hat{u}_A - \hat{t}_A \hat{t}_Q + \hat{s} \hat{s}_{AQ}) - 4\hat{u}_Q (\hat{s} + \hat{t}_A + \hat{u}_A) \right. \\ & \left. \left. - 2M_{Q_H}^2 \left( 2\hat{s} - \frac{\hat{t}_A}{M_{A_H}^2} (\hat{t}_A + \hat{u}_A) \right) \right] \right\} , \end{aligned} \quad (4)$$

where  $\hat{s} = (p_1 + p_2)^2$ ,  $\hat{t} = (p_1 - k_1)^2$ ,  $\hat{u} = (p_1 - k_2)^2$ , and  $\hat{s} + \hat{t} + \hat{u} = M_{Q_H}^2 + M_{A_H}^2$ . We have also introduced the following notations:  $\hat{t}_Q = \hat{t} - M_{Q_H}^2$ ,  $\hat{t}_A = \hat{t} - M_{A_H}^2$ ,  $\hat{u}_Q = \hat{u} - M_{Q_H}^2$ ,  $\hat{u}_A = \hat{u} - M_{A_H}^2$ , and  $\hat{s}_{AQ} = \hat{s} - M_{A_H}^2 - M_{Q_H}^2$ . In Eq.(4),  $g_s$  is the strong coupling constant and  $g_H = g' \tilde{Y}$  with  $g'$  and  $\tilde{Y}$  defined in [8]. The differential cross section for this subprocess is then given by

$$\frac{d\hat{\sigma}}{d\cos\theta^*} = \frac{\beta}{3072\pi} \frac{1}{\hat{s}} \sum |M|^2 , \quad (5)$$

where  $\theta^*$  is the scattering angle in the parton center-of-mass frame and  $\beta = [(1 - M_{Q_H}^2/\hat{s} - M_{A_H}^2/\hat{s})^2 - 4(M_{Q_H}^2/\hat{s})(M_{A_H}^2/\hat{s})]^{1/2}$ . Similar expression can be written down for  $\bar{q}g \rightarrow A_H \bar{Q}_H$  as well.

**B.  $gg, q\bar{q} \rightarrow Q_H \bar{Q}_H$**

The QCD production of the  $Q_H \bar{Q}_H$  pair is similar to the case of the top-quark pair. Feynman diagrams are depicted in Fig. 1(b). Hence the cross sections can be easily adapted

from previous calculations. The differential cross sections for these subprocesses are given by [12]

$$\frac{d\hat{\sigma}}{d\hat{t}}(q\bar{q} \rightarrow Q_H \bar{Q}_H) = \frac{8\pi\alpha_s^2}{9\hat{s}^2} \left[ \frac{1}{2} - v + z \right], \quad (6)$$

$$\frac{d\hat{\sigma}}{d\hat{t}}(gg \rightarrow Q_H \bar{Q}_H) = \frac{\pi\alpha_s^2}{12\hat{s}^2} \left( \frac{4}{v} - 9 \right) \left[ \frac{1}{2} - v + 2z \left( 1 - \frac{z}{v} \right) \right], \quad (7)$$

where  $z = M_{Q_H}^2/\hat{s}$  and  $v = (\hat{t} - M_{Q_H}^2)(\hat{u} - M_{Q_H}^2)/\hat{s}^2$ . In the above cross section for  $q\bar{q} \rightarrow Q_H \bar{Q}_H$ , we have neglected the contribution from an  $A_H$  exchange in the  $t$ -channel. Compared with the QCD diagram, this contribution is suppressed by the weak coupling  $g_H^2$  as well as the heavy mass effect in the propagator of  $A_H$ . The above cross sections of various parton-level subprocesses are convoluted with the parton distribution functions to obtain the monojet and dijet cross sections at hadron colliders. We will return to this at Section IV.

### III. COANNIHILATION CROSS SECTIONS AND THE COUPLING $g_H$

The most recent WMAP data [1] can give us some crude estimation of the coupling  $g_H$ . We will focus at the coannihilation region where  $M_{Q_H}$  is close to the LTP mass  $M_{A_H}$ . The relevant annihilation processes are  $A_H A_H \rightarrow f \bar{f}$  with  $f$  stands for either a lepton or a quark,  $Q_H \bar{Q}_H \rightarrow q\bar{q}, gg$ , and  $A_H Q_H (\bar{Q}_H) \rightarrow q(\bar{q})g$ . Their matrix elements can be easily obtained and are listed as below.

**A.**  $A_H(k_1)A_H(k_2) \rightarrow f(p_1)\bar{f}(p_2) :$

$$\begin{aligned} \overline{\sum} |M|^2 = & \frac{1}{9} g_H^2 N_c^2 \left\{ \frac{1}{\hat{t}_Q^2} \left[ \hat{t}(7\hat{t} + 4\hat{u}) - 4M_{A_H}^4 - 4 \frac{\hat{t}^2(\hat{t} + \hat{u})}{M_{A_H}^2} + \frac{\hat{t}^3 \hat{u}}{M_{A_H}^4} \right] \right. \\ & + \frac{1}{\hat{u}_Q^2} \left[ \hat{u}(7\hat{u} + 4\hat{t}) - 4M_{A_H}^4 - 4 \frac{\hat{u}^2(\hat{t} + \hat{u})}{M_{A_H}^2} + \frac{\hat{t} \hat{u}^3}{M_{A_H}^4} \right] \\ & \left. - \frac{2}{\hat{t}_Q \hat{u}_Q} \left[ 7\hat{t}\hat{u} + 8M_{A_H}^2(\hat{t} + \hat{u}) - 16M_{A_H}^4 - 4 \frac{\hat{t}\hat{u}(\hat{t} + \hat{u})}{M_{A_H}^2} + \frac{\hat{t}^2 \hat{u}^2}{M_{A_H}^4} \right] \right\}, \quad (8) \end{aligned}$$

where  $N_c = 1$  or  $3$  for  $f$  equals a lepton or a quark, respectively. Here the subscript label  $Q$  can be referred to the heavy lepton or quark depends on whether  $f$  is a lepton or a quark.

**B.**  $Q_H(k_1)\bar{Q}_H(k_2) \rightarrow q(p_1)\bar{q}(p_2) :$

$$\begin{aligned} \overline{\sum}|M|^2 = & \left(\frac{1}{2N_c}\right)^2 \left\{ 8g_s^4 \frac{(N_c^2 - 1)^2}{4} \frac{1}{\hat{s}^2} [\hat{t}_Q^2 + \hat{u}_Q^2 + 2M_{Q_H}^2 \hat{s}] \right. \\ & + g_H^4 N_c^2 \frac{1}{\hat{t}_A^2} \left[ 4(\hat{s} + \hat{t}_Q)^2 + 4 \frac{M_{Q_H}^4 \hat{s}}{M_{A_H}^2} + \frac{M_{Q_H}^4 \hat{t}_Q^2}{M_{A_H}^4} \right] \\ & \left. - 2g_H^2 g_s^2 \frac{N_c^2 - 1}{2} \frac{1}{\hat{s}\hat{t}_A} \left[ 4(\hat{s} + \hat{t}_Q)^2 + 4M_{Q_H}^2 \hat{s} + 2 \frac{M_{Q_H}^2}{M_{A_H}^2} (\hat{t}_Q^2 + M_{Q_H}^2 (\hat{s} + \hat{t})) \right] \right\}. \end{aligned} \quad (9)$$

**C.**  $Q_H(k_1)\bar{Q}_H(k_2) \rightarrow g(p_1)g(p_2) :$

$$\overline{\sum}|M|^2 = \left(\frac{1}{2N_c}\right)^2 \frac{64}{3} g_s^4 (1 - 4z) \left(\frac{4}{v} - 9\right) \left[\frac{1}{2} - v + 2z \left(1 - \frac{z}{v}\right)\right], \quad (10)$$

where  $z$  and  $v$  are defined as those after Eq.(7).

**D.**  $A_H(k_1)Q_H(k_2) \rightarrow q(p_1)g(p_2)$  **and**  $A_H(k_1)\bar{Q}_H(k_2) \rightarrow \bar{q}(p_1)g(p_2)$

$$\overline{\sum}|M|^2 = \frac{1}{3} \frac{1}{2N_c} \text{Eq.(4)}. \quad (11)$$

### E. Estimation of $g_H$

A useful formula for estimating the relic density of a weakly-interacting massive particle is given by [13]

$$\Omega_\chi h^2 \approx \frac{0.1 \text{ pb}}{\langle \sigma v \rangle}. \quad (12)$$

The most recent result from WMAP is [1]

$$\Omega_{\text{CDM}} h^2 = 0.105 \pm 0.009, \quad (13)$$

where we have used the WMAP-data-only fit and taken  $\Omega_{\text{CDM}} = \Omega_{\text{matter}} - \Omega_{\text{baryon}}$ . Using Eq.(12), one can translate this WMAP data to  $\langle \sigma v \rangle$

$$\langle \sigma v \rangle \approx 0.95 \pm 0.08 \text{ pb}. \quad (14)$$

The effective annihilation cross section due to coannihilation can be written as

$$\langle \sigma_{\text{eff}} v \rangle = \sum_{ij} \langle \sigma_{ij} v_{ij} \rangle \frac{n_i^{\text{eq}} n_j^{\text{eq}}}{n^2},$$

where  $n = \sum_i n_i^{\text{eq}}$  and the equilibrium number density  $n_i^{\text{eq}}$  of each species  $i$  is given by

$$n_i^{\text{eq}} \sim g_i \left( \frac{m_i T}{2\pi} \right)^{3/2} e^{-m_i/T},$$

where  $g_i$  is the spin degree of freedom of the species  $i$ . The relative velocity  $v_{ij}$  is

$$v_{ij} = \frac{\sqrt{(p_i \cdot p_j)^2 - m_i^2 m_j^2}}{E_i E_j},$$

where  $E_i$  and  $p_i$  are the energy and 4-momenta of the species  $i$ , respectively. In the center-of-mass frame of  $(i, j)$ , the relative velocity  $v_{ij}$  in the non-relativistic limit can be simplified to

$$v_{ij} = \frac{2\lambda^{1/2}(1, m_i^2/s, m_j^2/s)}{1 + \mathcal{O}(m_i^4/s^2)} \approx 2\lambda^{1/2}(1, m_i^2/s, m_j^2/s), \quad (15)$$

where  $\lambda(1, m_i^2/s, m_j^2/s) = (1 - m_i^2/s - m_j^2/s)^2 - 4(m_i^2/s)(m_j^2/s)$ .

In the present coannihilation scenario, we assume that there are 5 flavors of heavy quarks (from the heavy partners of the first two generation quarks and the partner of the  $b$ -quark of the third generation). The resultant effective annihilation cross section is given by

$$\begin{aligned} \langle \sigma_{\text{eff}} v \rangle = & \frac{1}{\left[ 1 + 10 \frac{g_{Q_H}}{g_{A_H}} \left( 1 + \frac{\Delta m}{M_{A_H}} \right)^{3/2} e^{-\Delta m/T} \right]^2} \left\{ 5 \sigma_{A_H A_H \rightarrow q\bar{q}} v_{A_H A_H} \right. \\ & + 10 \sigma_{A_H Q_H \rightarrow qg} v_{A_H Q_H} \left( \frac{g_{Q_H}}{g_{A_H}} \right) \left( 1 + \frac{\Delta m}{M_{A_H}} \right)^{3/2} e^{-\Delta m/T} \\ & \left. + 5 \left( \sigma_{Q_H \bar{Q}_H \rightarrow q\bar{q}} + \sigma_{Q_H \bar{Q}_H \rightarrow gg} \right) v_{Q_H \bar{Q}_H} \left( \frac{g_{Q_H}}{g_{A_H}} \right)^2 \left( 1 + \frac{\Delta m}{M_{A_H}} \right)^3 e^{-2\Delta m/T} \right\}, \quad (16) \end{aligned}$$

where  $\Delta m = M_{Q_H} - M_{A_H}$ ,  $g_{Q_H} = 2$ ,  $g_{A_H} = 3$ , and  $\sigma_{ij}$  is the annihilation cross section between species  $i$  and  $j$ . We have assumed that twice the mass of the LTP  $A_H$  is far away enough from the Higgs pole, then only the coannihilation processes listed in this Section are important. The coannihilation cross sections can be obtained from the amplitude-squared listed in Eqs. (8), (9), (10), and (11). Taking the simple approximations that the freeze-out temperature occurs at  $T_f \approx M_{A_H}/25$  and during the freeze-out the species have a relative velocity  $\beta = \lambda^{1/2}(1, M_{A_H}^2/s, M_{Q_H}^2/s) \approx 0.3$ , we ignore the thermal average and evaluate the quantity  $\sigma_{\text{eff}} v$  directly from Eqs.(16) and (8)–(11) as a function of three parameters  $g_H$ ,

Contour plot of  $\sigma v = 0.95 \pm 0.08$  pb in the  $(\Delta m / (\text{GeV}), g_H)$  plane

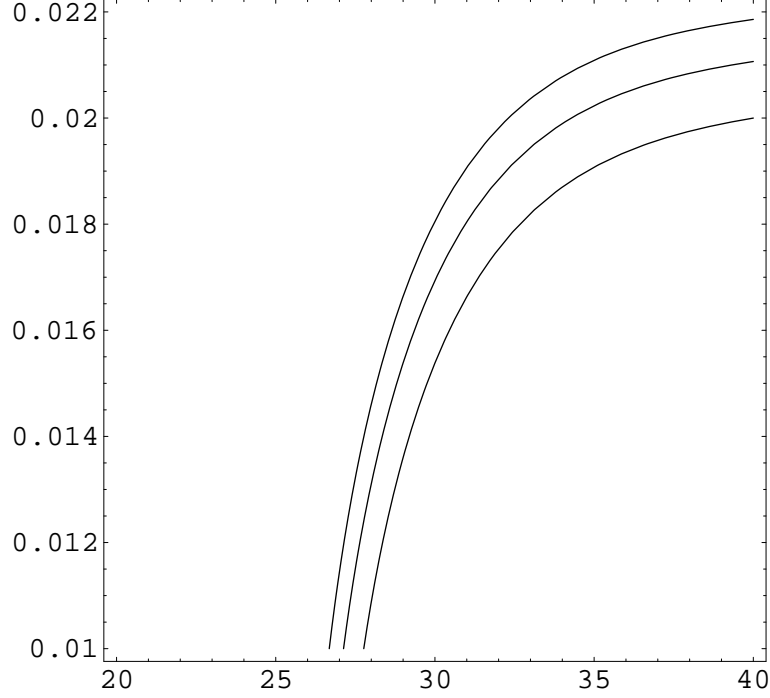


FIG. 2: The contour plot of coannihilation cross section  $\sigma_{\text{eff}} v$  in the plane of  $(\Delta m, g_H)$ . We take  $M_{A_H} = 200$  GeV. The WMAP implied result of  $0.95 \pm 0.08$  pb for this quantity is shown.

$\Delta m \equiv M_{Q_H} - M_{A_H}$ , and  $M_{A_H}$ . In Fig. 2, we show the contours of  $\sigma_{\text{eff}} v = 0.95 \pm 0.08$  pb in the plane of  $(\Delta m, g_H)$  for the case  $M_{A_H} = 200$  GeV. From the figure, it is interesting to see that when  $\Delta m$  increases along the contour, the required  $g_H$  has to increase so as to come up with sufficient coannihilation rate. For a reasonable  $\Delta m \lesssim 30$  GeV and  $M_{A_H}$  in the range varies from 200 to 400 GeV,  $g_H$  never gets larger than 0.02. It is obvious that these values of  $g_H$  is too small to achieve a meaningful production cross section for  $A_H Q_H$  at colliders, and thus a negligible signal of monojet plus missing energy. We therefore focus on the dijet plus missing energy signal, which is independent of  $g_H$ , in the next Section.

#### IV. HADRONIC PRODUCTION

In the coannihilation region,  $Q_H$  decays predominantly into  $A_H q$ . Its decay rate is given by

$$\Gamma(Q_H \rightarrow A_H q) = \frac{1}{32\pi} g_H^2 M_{Q_H} \left( 2 + \frac{M_{Q_H}^2}{M_{A_H}^2} \right) \left( 1 - \frac{M_{A_H}^2}{M_{Q_H}^2} \right)^2. \quad (17)$$

Since this is the only possible decay mode of  $Q_H$  in this region, its branching ratio into a jet plus missing energy is 100%. The decay time calculated using the above formula is so short that the decay is actually prompt. In the rest frame of  $Q_H$ , the available energy to the jet depends on the mass difference  $M_{Q_H} - M_{A_H} \sim 20$  GeV, which is not so small.

In the production of  $A_H Q_H$ , the final state has only one jet with missing transverse energy. In this monojet signal, the  $p_{T_j}$  of the jet is the same as the missing transverse momentum  $\cancel{p}_T$ . Although the monojet plus missing energy signal is very clean, there are still a handful of SM backgrounds one needs to contemplate. The major SM background comes from  $Z + 1j$  production followed by the invisible decay of the  $Z$  boson. Unfortunately, we cannot use the recoil mass information of the monojet to reject this  $Z + 1j$  background in the hadronic environment. The other reducible monojet SM background comes from, for example,  $W + 1j \rightarrow \ell \nu + 1j$  with the charged lepton unidentified. With the small value of  $g_H$  obtained in the last Section, the production cross section of  $A_H Q_H$  is too small compared with the  $Z + 1j \rightarrow 1j + \cancel{p}_T$  background. In the following, we focus on the direct production of  $Q_H \bar{Q}_H$  which gives rise to dijet plus missing energy signal.

In the production of  $Q_H \bar{Q}_H$ , the final state consists of two jets with missing transverse energy. The corresponding major SM background is  $Z + 2j$  production with  $Z \rightarrow \nu \bar{\nu}$ . This SM background has been studied in great details by experimental collaborations [14] and by theoretical calculations [15]. We use MADGRAPH [16] to generate the helicity amplitudes of the tree-level  $Z + 2j$  background, followed by  $Z \rightarrow \nu \bar{\nu}$  decay. We impose the following acceptance cuts for the jets:

$$p_{T_j} > 20 \text{ GeV}, \quad |y_j| < 1.5, \quad \text{and} \quad \Delta R_{jj} > 0.7, \quad (18)$$

where  $p_{T_j}$  is the transverse momentum,  $y_j$  is the rapidity, and  $\Delta R = \sqrt{(\Delta y)^2 + (\Delta \phi)^2}$  denotes the spatial separation of the two jets with  $\Delta y$  and  $\Delta \phi$  denote the differences in their rapidities and azimuth angles, respectively.

In Fig. 3, we show the production rate for the dijet plus missing energy signal with the

acceptance cuts defined in Eq. (18) as a function of  $M_{Q_H}$ . The spectra of the transverse momentum of the jets and the missing transverse momentum for the dijet plus missing energy signal and the  $Z + 2j \rightarrow 2j + \cancel{p}_T$  background at the Tevatron and at the LHC are shown in Figs. 4 and 5, respectively. We have included 5 degenerate flavors of  $Q_H$  in the signal, and multiplied the SM background rate by the branching ratio  $B(Z \rightarrow \nu\bar{\nu}) = 0.2$  to obtain the  $Z + 2j \rightarrow 2j + \cancel{p}_T$  background. It is clear that the spectra for the Little Higgs dark matter model are softer than those from the background, reflecting the fact that the mass difference  $\Delta m = M_{Q_H} - M_{A_H}$  is relatively small in the coannihilation region. Note that this soft region in the missing transverse momentum spectra overlaps with the Jacobian peak of the  $Z$  from the SM background. However, the SM  $Z + 2j$  background can be measured with high accuracy using  $\ell^+\ell^- + 2j$  mode. The  $Z + 2j \rightarrow 2j + \cancel{p}_T$  can then be obtained quite reliably by using both the leptonic and invisible branching ratios of the  $Z$  boson. One therefore should be able to quantify the SM background of  $2j + \cancel{p}_T$  with high accuracy. By measuring the  $p_T$  spectra of the jets at the low end accurately and/or any distortion around the Jacobian peak in the missing transverse momentum spectra of the dijet precisely, one could identify the existence of the dijet signal from the Little Higgs dark matter model at the coannihilation region.

## V. CONCLUSIONS

Little Higgs models with  $T$ -parity provide the weakly interacting particle  $A_H$  as the lightest  $T$ -odd particle to be an interesting alternative candidate for the dark matter in the Universe. We have pointed out a potentially novel signature in the direct production of  $Q_H\bar{Q}_H$  in the Little Higgs models with  $T$ -parity in the coannihilation region where  $M_{Q_H} - M_{A_H} \lesssim 20$  GeV. It gives rise to dijet plus missing energy events at the Tevatron and at the LHC, which is potentially discoverable despite the SM background of  $Z + 2j \rightarrow 2j + \cancel{p}_T$ . Note that the associated production of  $Q_H A_H$ , which gives rise to a cleaner monojet +  $\cancel{E}_T$  signature, is unfortunately very tiny because of the small value of the coupling  $g_H$  constrained by the WMAP data.

We close by reiterating that one may use the monojet plus missing energy signature to at least partially distinguish Little Higgs models with  $T$ -parity from the minimal SUSY models. SUSY events tend to give multijet ( $> 2$ ) plus missing energy events from the QCD

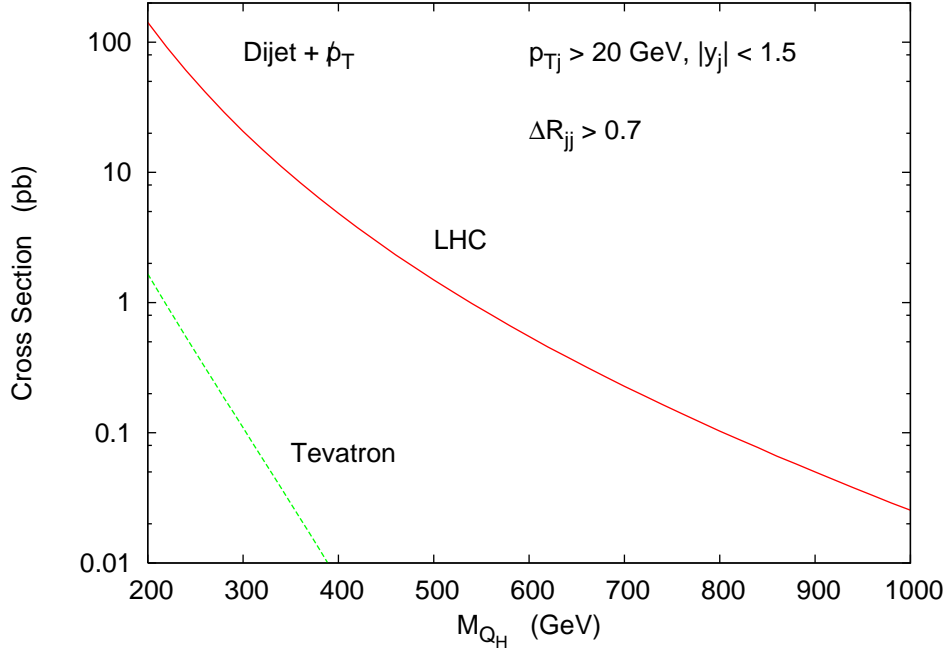


FIG. 3: Production rate for the dijet plus missing energy signal with the acceptance cuts defined in Eq. (18) at the Tevatron and at the LHC.

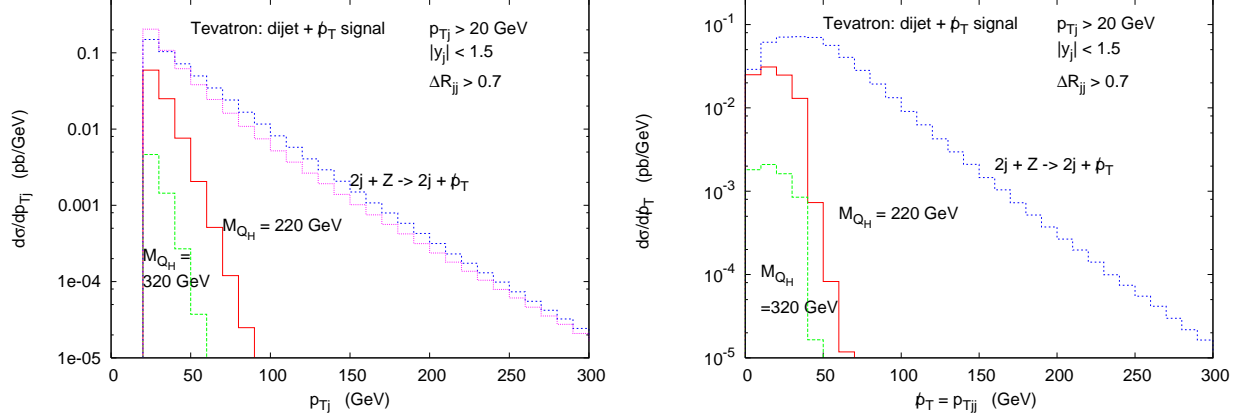


FIG. 4: The differential cross section versus (a) the transverse momentum of the jets and (b) the missing transverse momentum for the dijet +  $\cancel{p}_T$  signal and the  $Z + 2j \rightarrow 2j + \cancel{p}_T$  background at the Tevatron. We have used 2 sets of  $(M_{Q_H}, M_{A_H}) = (220, 200)$  and  $(320, 300)$  GeV.

production of  $\tilde{g}\tilde{g}$ ,  $\tilde{q}\tilde{q}^*$ , and  $\tilde{g}\tilde{q}(\tilde{q}^*)$ . On the other hand, the dominant production for  $T$ -odd particles are  $gg, q\bar{q} \rightarrow Q_H\bar{Q}_H$  and  $gq \rightarrow Q_H A_H$ , which give rise to dijet and monojet, respectively, plus missing energy events. Therefore, by counting how many jets in multijet plus missing energy events, one may be able to differentiate between Little Higgs models

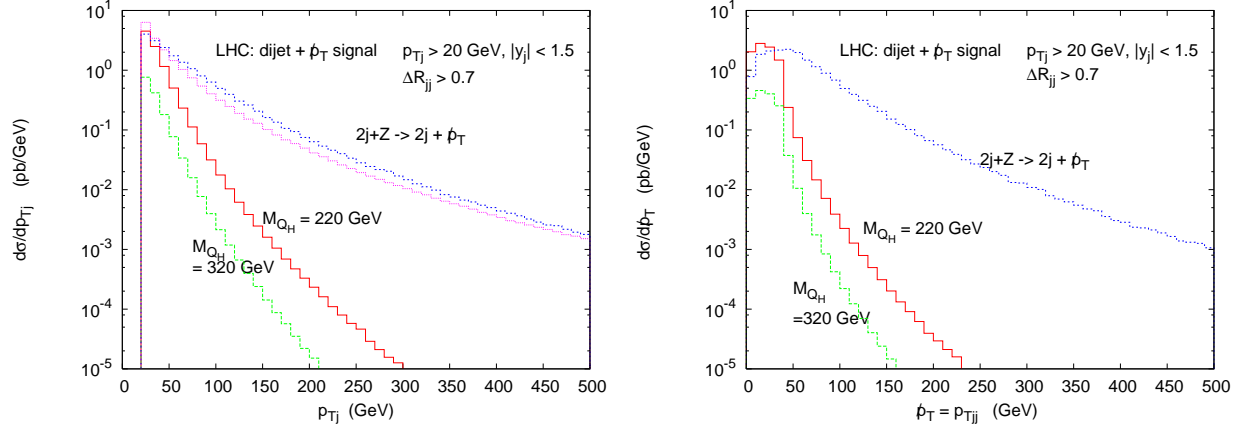


FIG. 5: The differential cross section versus (a) the transverse momentum of the jets and (b) the missing transverse momentum for the dijet +  $\cancel{p}_T$  signal and the  $Z + 2j \rightarrow 2j + \cancel{p}_T$  background at the LHC. We have used 2 sets of  $(M_{Q_H}, M_{A_H}) = (220, 200)$  and  $(320, 300)$  GeV.

with  $T$ -parity and minimal SUSY models.

### Acknowledgment

This research was supported in part by the National Science Council of Taiwan R. O. C. under Grant Nos. NSC 94-2112-M-007-010-, and by the National Center for Theoretical Sciences.

- 
- [1] D. N. Spergel *et al.*, [arXiv:astro-ph/0603449].
  - [2] M. Schmaltz and D. Tucker-Smith, Ann. Rev. Nucl. Part. Sci. **55**, 229 (2005) [arXiv:hep-ph/0502182] ; M. Perelstein, [arXiv:hep-ph/0512128] and references therein.
  - [3] H. C. Cheng and I. Low, JHEP **0309**, 051 (2003) [arXiv:hep-ph/0308199].
  - [4] H. C. Cheng and I. Low, JHEP **0408**, 061 (2004) [arXiv:hep-ph/0405243].
  - [5] I. Low, JHEP **0410**, 067 (2004) [arXiv:hep-ph/0409025].
  - [6] M. Asano, S. Matsumoto, N. Okada, and Y. Okada, [arXiv:hep-ph/0602157].
  - [7] A. Martin, [arXiv:hep-ph/0602206].
  - [8] A. Birkedal, A. Noble, M. Perelstein, and A. Spray, [arXiv:hep-ph/0603077].

- [9] C. Csaki, J. Hubisz, G. D. Kribs, P. Meade, and J. Terning, Phys. Rev. D **67**, 115002 (2003) [arXiv:hep-ph/0211124].
- [10] H. C. Cheng, I. Low, and L. T. Wang, [arXiv:hep-ph/0510225]; J. Hubisz and P. Meade, Phys. Rev. D **71**, 035016 (2005) [arXiv:hep-ph/0411264]; J. Hubisz, P. Meade, A. Noble, and M. Perelstein, JHEP **0601**, 135 (2006) [arXiv:hep-ph/0506042]; C. O. Dib, R. Rosenfeld, and A. Zerwekh, [arXiv:hep-ph/0509179]; J. Hubisz, S. J. Lee, and G. Paz, [arXiv:hep-ph/0512169]; C. R. Chen, K. Tobe, and C. P. Yuan, [arXiv:hep-ph/0602211]; M. Blanke, A. J. Buras, A. Poschenrieder, C. Tarantino, S. Uhlig, and A. Weiler, [arXiv:hep-ph/0605214].
- [11] T. Han, H. E. Logan, B. McElrath, and L. T. Wang, Phys. Rev. D **67**, 095004 (2003) [arXiv:hep-ph/0301040].
- [12] K. m. Cheung, Phys. Rev. D **53**, 3604 (1996) [arXiv:hep-ph/9511260]; P. Haberl, O. Nachtmann, and A. Wilch, Phys. Rev. D **53**, 4875 (1996) [arXiv:hep-ph/9505409].
- [13] G. Bertone, D. Hooper, and J. Silk, Phys. Rept. **405**, 279 (2005) [arXiv:hep-ph/0404175].
- [14] “Search for extra dimensions in Run II jets plus missing  $E_T$  sample”, CDF public note 7986, [http://www-cdf.fnal.gov/physics/exotic/r2a/20050901.LED\\_JetMet/](http://www-cdf.fnal.gov/physics/exotic/r2a/20050901.LED_JetMet/); “Search for large extra spatial dimensions in jets plus missing  $E_T$  topologies”, DØ note DØ -CONF 4400.
- [15] J. Campbell, R. K. Ellis, and D. L. Rainwater, Phys. Rev. D **68**, 094021 (2003) [arXiv:hep-ph/0308195]; see also the website: <http://mcfm.fnal.gov>.
- [16] F. Maltoni and T. Stelzer, JHEP **0302**, 027 (2003) [arXiv:hep-ph/0208156].